Quantification of the cryoablation zone demarcated by pre- and postprocedural electroanatomic mapping in patients with atrial fibrillation using the 28-mm second-generation cryoballoon

David N. Kenigsberg, MD, FHRS,[*] Natalia Martin, BS,[1†] Hae W. Lim, PhD,[‡] Marcin Kowalski, MD, FHRS,[§] Kenneth A. Ellenbogen, MD, FHRS[‖]

From the [*]Florida Heart Rhythm Specialist, Plantation, Florida, [†]St Jude Medical, Inc, St Paul, Minnesota, [‡]Medtronic, Inc, Mounds View, Minnesota, [§]Staten Island University Hospital, Staten Island, New York, and [‖]Virginia Commonwealth University School of Medicine, Richmond, Virginia.

BACKGROUND There are 2 Food and Drug Administration–approved catheters (ThermoCool RF and Arctic Front Advance cryoballoon) for the treatment of drug refractory and symptomatic paroxysmal atrial fibrillation. Each tool is used to ablate the area surrounding the pulmonary veins (PVs). However, no study has described and quantified the ablated surface area after the application of cryoablation lesions with the second-generation cryoballoon.

OBJECTIVE The purpose of this study was to determine the area of ablation during cryoballoon PV isolation.

METHODS Preprocedural computed tomography angiography of the left atrium (LA) was conducted in 43 patients to accurately determine spatial chamber dimensions. Before and after the ablation procedure, a detailed 3-dimensional electroanatomic map of the LA was created and merged onto the computed tomography angiogram to improve the accuracy of the data recordings.

RESULTS The posterior LA wall had a mean surface area of 31.1 (±1.6 SEM) cm^2. Left- and right-sided antral PV surface areas of cryoballoon ablation were not statistically different ($P = .935$), which were 11.4 (±0.8 SEM) and 11.3 (±0.8 SEM) cm^2, respectively. In total, 27% of the posterior LA wall remained unablated, electrically functional, and homogeneous with regard to voltage conductivity. This ablation strategy resulted in 95.3% freedom from atrial fibrillation at 6 months.

CONCLUSION The area of the posterior LA wall ablation with the cryoballoon catheter is wide and antral, and the resulting posterior LA wall debulking could be a part of the cryoballoon efficacy beyond discrete PV isolation.

KEYWORDS Atrial fibrillation; Catheter ablation; Cryoballoon; Cryoablation; Radiofrequency ablation; Wide area circumferential ablation

ABBREVIATIONS 3D EAM = 3-dimensional electroanatomic map; **AF** = atrial fibrillation; **ANOVA** = analysis of variance; **CTA** = computed tomography angiography; **eCRF** = electronic case report form; **LA** = left atrium/atrial; **LIPV** = left inferior pulmonary vein; **LSPV** = left superior pulmonary vein; **PNI** = phrenic nerve injury; **PV** = pulmonary vein; **PVI** = pulmonary vein isolation; **RIPV** = right inferior pulmonary vein; **RSPV** = right superior pulmonary vein; **WACA** = wide area circumferential ablation

(Heart Rhythm 2015;12:283–290)

Introduction

Catheter ablation therapy has been given the highest level recommendation (class I, level A) for the treatment of drug refractory and symptomatic paroxysmal atrial fibrillation (AF) in the latest American College of Cardiology/American Heart Association guidelines.[1–3] A cornerstone of AF ablation procedures is electrical isolation of the pulmonary veins (PVs) by ablation lesions around the PVs.[4] Haïssaguerre et al[4] originally described muscular sleeves around the PV that are arrhythmogenic and are involved in the initiation and maintenance of AF. Since the original description, variations of this technique have included wide area circumferential ablation (WACA) and pulmonary vein antrum ablation/isolation. In addition, circular-architecture ablation catheters have been designed with the intent of performing pulmonary vein isolation (PVI) through the simultaneous delivery of ablative energy, which are sometimes referred to as "single-shot" ablation catheters.

The cryoballoon catheter (Arctic Front Advance, Medtronic, Inc, Minneapolis, Minnesota) is an anatomically based ablation device that allows for simplified PVI with a favorable safety profile.[5] In practice, the cryoballoon catheter

Address reprint requests and correspondence: Dr David N. Kenigsberg, Florida Heart Rhythm Specialist, 350 NW 84th Avenue, Suite 110, Plantation, FL 33324. E-mail address: dkenigsb@yahoo.com.

[1]Ms Martin is an employee of St Jude Medical. Dr Lim is an employee of Medtronic.

is apposed against the atrial tissue surrounding the PV ostium, resulting in cryothermal energy delivery to the contacting atrial tissue and ultimately the formation of a lesion.[6] Given the spherical nature of the cryoballoon and size mismatch of the balloon to the PV orifice, quite often the balloon is in physical contact with adjacent atrial tissue away from the PV orifice, creating a WACA as a common lesion set.

With regard to ablation lesion(s) description and assessment, 3-dimensional electroanatomic maps (3D EAMs) have proved to be useful for measuring local voltage abnormalities and they use this information as a surrogate for healthy vs scarred (ablated) tissue.[7–9] Also, previous correlations between regions of cardiac scar (ablation) and low voltage have been demonstrated.[10–12] Scar burden has been used to predict ablation efficacy,[13,14] stroke risk,[15] and, more recently, the site of PV reconnection in patients who have undergone initial AF ablation, but had a recurrence of arrhythmia.[16] The extension of the scar (ablated cardiac tissue) created by the cryoballoon during PVI had not been previously studied with the second-generation cryoballoon. Therefore, we attempted to calculate the area of acute ablation produced after PVI using the cryoballoon catheter that extends beyond the PV orifice. In this study, we compared the area of healthy tissue and ablation injury before and after cryoablation.

Methods

This study examined 43 consecutive cryoballoon procedures that encompassed a period of 6 months (October 15, 2013, to April 11, 2014), and all patients were treated with the 28-mm second-generation cryoballoon. The study design was a single-arm, single-center, prospective collection of data recorded in the electronic case report form (eCRF). All patients were symptomatic and drug refractory with a history of AF. Informed consent was obtained, and local institutional review board approval was granted. The procedures performed in this study were standard of care during the time period of data collection.

Patient selection

Inclusion criteria for these 43 patients required a clinical history of symptomatic AF, 1-drug refractory treatment of AF, and AF ablation by PVI using a cryoballoon catheter. Exclusion criteria were patients younger than 18 years, patients older than 90 years, patients who have undergone AF catheter ablation, patients undergoing extensive left atrial (LA) substrate modification instead of PVI (including complex fractionated atrial electrogram ablation, focal impulse and rotor modulation ablation, ablative isolation of the LA appendage, or autonomic denervation via posterior LA wall ablation), or patients with permanent AF.

3D EAM and cryoballoon ablation

All the cryoballoon ablation procedures were conducted by a single experienced operator with more than 200 cryoablation procedures at the time of this study. The procedural techniques and methods for cryoballoon ablation have been previously described in detail,[5,17] and our own cryoablation procedure was similar to those of published reports. In brief, preprocedural cardiac computed tomography angiography (CTA) was conducted in all 43 patients. On the day of ablation, transesophageal echocardiography was routinely conducted to assess the LA for thrombus, chamber size/dimensions, and anatomical structures. Typically, an intracardiac echocardiography catheter was used to visualize and guide transseptal needle entry into the LA chamber.

Using CTA as guidance, a conventional 20-pole circular diagnostic mapping catheter was advanced into each PV to obtain baseline electrical information. The EnSite NavX system (St Jude Medical, Inc) was used to create an electrical impedance–based map of the entire LA surface. Specifically, electroanatomic bipolar voltage-amplitude substrate mapping was completed with a minimum point setting at 100 mV and a 2 mV demarcation for healthy tissue. After the completion of electroanatomic mapping, the 3D EAM was merged onto the CTA rendering.

Next, the cryoballoon catheter (28 mm, Arctic Front Advance) and the sheath were delivered into the LA using a J-tip guidewire or the Achieve inner lumen mapping catheter (Achieve™ Mapping Catheter; Medtronic, Inc., Minneapolis, Minnesota). The balloon was advanced toward the PV ostium and inflated. Cryoballoon-to-PV occlusion was tested with the retention/leakage of contrast agent after injection at the distal tip of the balloon. Subsequent to occlusion verification, a minimum of 2 freezes were delivered to each PV with a targeted duration of 180 seconds. After the completion of the ablation procedure, entrance and exit block testing was used to confirm PVI at each PV.

Then, postablation 3D electroanatomic mapping was performed to assess voltage and ablation border demarcation, as described previously.[18,19] Briefly, the proximal border of PVI was denoted when there was a complete elimination of electrograms, and this was assessed with the 3D EAM by withdrawing the circular mapping catheter from the PV toward the venoatrial junction. The PV ostium was assessed by using the CTA-3D EAM merged image, and it was located by the steep angle of change between the LA wall and the tubular aspect of the PV. Precise spatial/electrical measurements were mapped and recorded with the EnSite NavX system (Figure 1). After each ablation procedure, measurements of pre- and postablation dimensions were recorded in the eCRF.

Data recordings

Data that were recorded in the eCRF included LA volume measurements, posterior LA wall surface area, and distances to postablation lesions (at the superior and inferior margins of each PV). As demonstrated in Figures 1–3, these measurements (from the CTA-3D EAM merged image) were used to calculate pre- and postablation surface areas in the LA. Each distance measurement was recorded twice by 2 separate

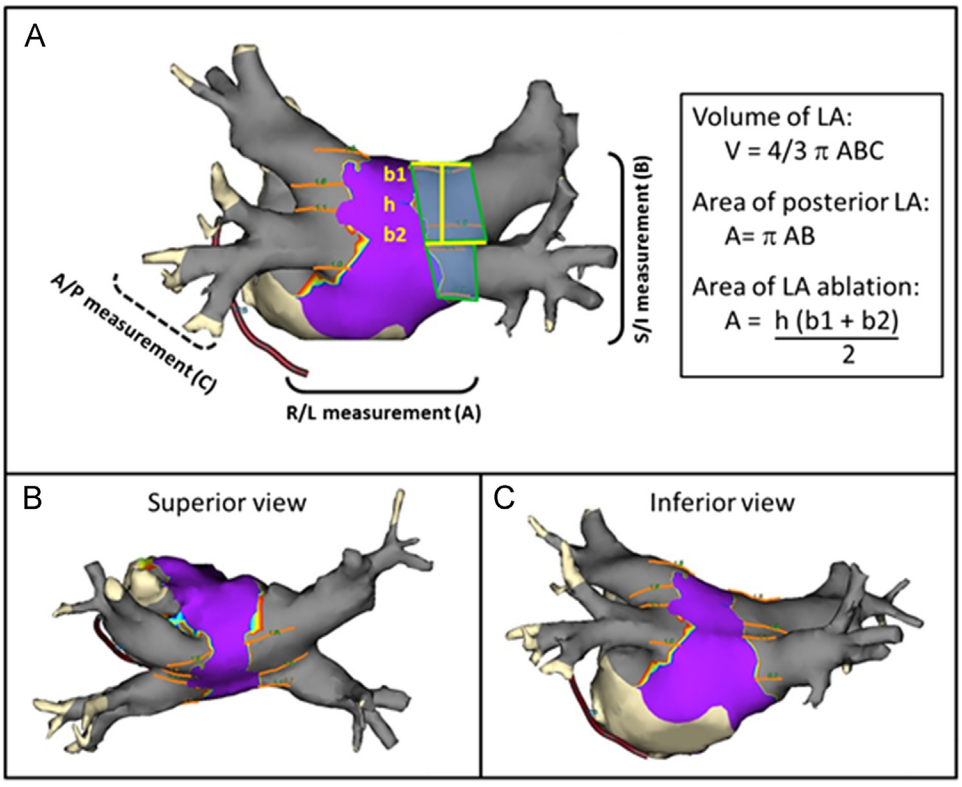

Figure 1. Measurements of the left atrial (LA) dimensions recorded using the EnSite NavX system. The scale on the NavX voltage map was set from 0.2 to 1.2 mV. The purple region represents voltage > 1.2 mV, and the gray region represents voltage < 0.2 mV. **A:** Measurement system and mathematical formulas used to calculate volumes and areas. The green transparent trapezoids demarcate the areas of right-sided ablation in this patient. Orange lines are recorded distances measured with the NavX system. Yellow lines represent the measurements used to calculate the right superior pulmonary vein area of ablation. **B and C:** Superior and inferior views of the same LA demonstrate the placement of measurements that were recorded. A/P = anterior/posterior, R/S = right/left; S/I = superior/inferior.

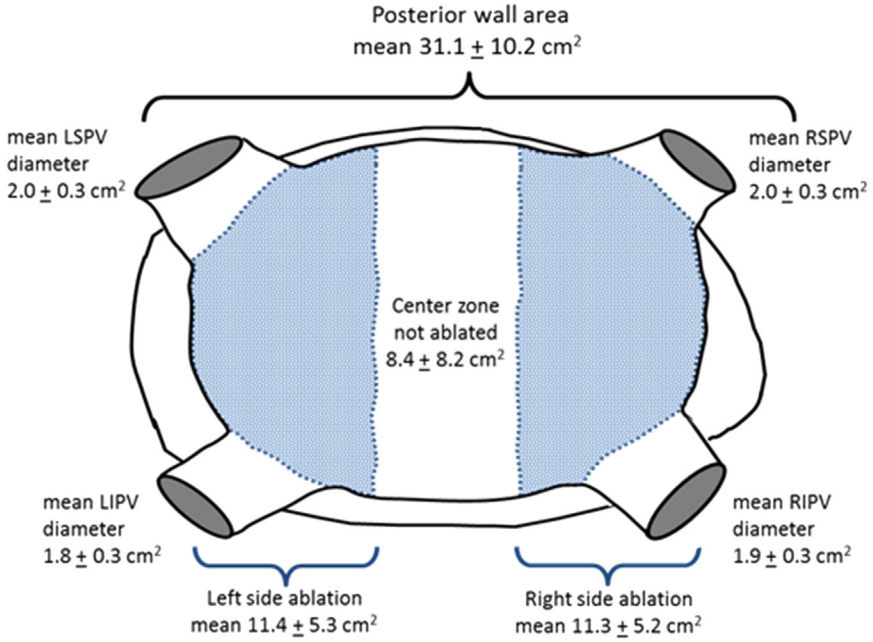

Figure 2 Area of cryoballoon ablation in the left atrium (LA). A schematic depiction of the LA, with measurements and values reported. The blue-dotted zone represents the cryoballoon ablated area. Numerical values are mean ± SD. LIPV = left inferior pulmonary vein; LSPV = left superior pulmonary vein; RIPV = right inferior pulmonary vein; RSPV = right superior pulmonary vein.

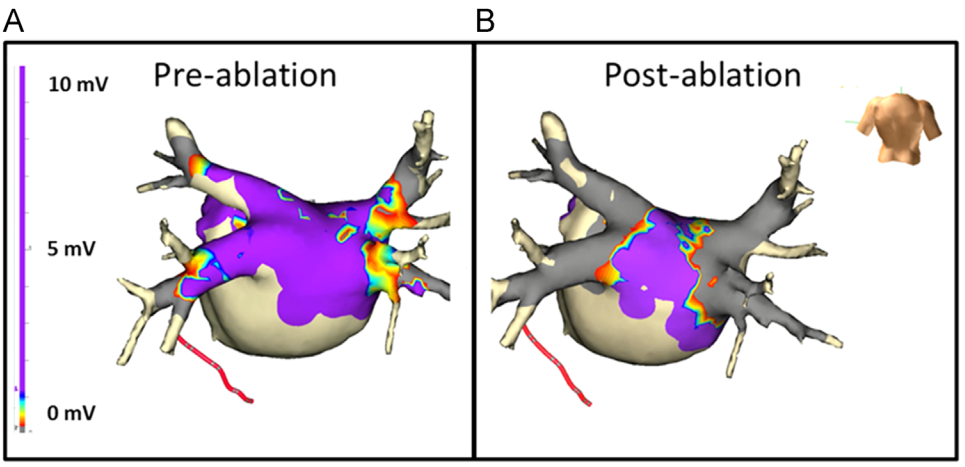

Figure 3 Pre- and postablation images recorded with the 3-dimensional electroanatomic mapping system. The scale on the NavX voltage map was set from 0.2 to 1.2 mV. The purple region represents voltage >1.2 mV, and the gray region represents voltage < 0.2 mV. **A:** A preablation voltage map demonstrating the posterior left atrial (LA) and 4 pulmonary veins. **B:** A postablation voltage map demonstrating cryoballoon lesion demarcation on the posterior LA wall.

investigators, and the 2 data records showed 90% reproducibility. When measurements were different, the mean distance (between the 2 investigators) was recorded. Anatomical cardiac measurements (Figure 1A) were made in accordance to previously published studies.[18,19] In brief, LA volume was calculated from anterior/posterior, right/left, and superior/inferior recorded data by using an ellipsoid model. The posterior wall surface area was calculated from right/left and superior/inferior measurements of the LA, and surface areas of left- and right-sided LA ablation procedures were calculated from distances to postablation lesion measurements by using a trapezoidal rule model.

Statistical analyses

All descriptive statistics are recorded as means with reported SEM and SD. Means are reported with the number of individual observations used to calculate each statistical parameter. For 2-sample comparisons of continuous variables, a Student *t* test was used to determine statistically significant interactions. When multiple samples were compared, an analysis of variance (ANOVA) test was used to examine whether populations were statistically different, and the outlier group(s) were identified within each table. Statistical significance was set at $P < .05$, and all statistical analyses were calculated using Minitab (Minitab, Inc.)

Results

Demographic data of the 43 consecutive patients enrolled in the study are given in Table 1. Table 2 lists the characteristics of cryoablation procedures used in this study. The mean number of cryoballoon freezes ranged from 2.0 (±0 SD) to 2.5 (±1.3 SD) applications per vein (median 2.0; mode 2.0). The mean number of right inferior pulmonary vein (RIPV) applications were found to be significantly higher using the ANOVA test ($P = .012$). The mean freeze duration per application was 169 (±29 SD), 178 (±10 SD), 159 (±38 SD), and 169 (±31 SD) seconds for the left superior pulmonary vein (LSPV), left inferior pulmonary vein (LIPV), right superior pulmonary vein (RSPV), and RIPV, respectively (median 180 seconds; mode 180 seconds). The mean freeze duration for the LIPV was found to be statistically longer and for the RSPV statistically shorter than that for the other PVs using the ANOVA test ($P = .001$). Typical (target) freeze times were 180 seconds, with shorter durations representing freeze terminations based on electrical isolation of the PVs, ultracold balloon nadir temperature (< −60°C), or an attempt to avoid collateral tissue freezing (eg, phrenic nerve). The mean freeze nadir temperatures were −47 (±7 SD), −45 (±7 SD), −48 (±7 SD), and −45 (±6 SD)°C for the LSPV, LIPV, RSPV, and RIPV, respectively (median −47°C; mode −48°C). The nadir temperatures recorded at the superior veins were found to be higher than those recorded at the inferior veins using the

Table 1 Demographic characteristics of the patients

Patient characteristic on the day of ablation	Mean	SEM	SD
Age (y)	63.3	2.0	12.9
% Paroxysmal AF	79.1	6.3	41.2
% Male	74.4	6.7	44.2
Left atrial volume (mL)	70.8	5.5	36.0
No. of PVs per patient	4.1	0.1	0.5
LSPV diameter (cm)	2.0	0.1	0.3
LIPV diameter (cm)	1.8	0.1	0.3
RSPV diameter (cm)	2.0	0.1	0.3
RIPV diameter (cm)	1.9	0.1	0.3
% presenting in NSR	72.1	6.9	45.4
% receiving AADs	86.1	5.4	35.1
No. of AADs	1.0	0.1	0.6
% receiving anticoagulant	90.7	4.5	29.4
% receiving aspirin	23.3	6.5	42.8
% receiving NOAC*	51.2	7.7	50.6
% receiving other†	7.0	3.9	25.8
% receiving warfarin	14.0	5.4	35.1

AAD = antiarrhythmic drug; AF = atrial fibrillation; LIPV = left inferior pulmonary vein; LSPV = left superior pulmonary vein; NOAC = novel oral anticoagulant; NSR = normal sinus rhythm; RIPV = right inferior pulmonary vein; RSPV = right superior pulmonary vein.

*NOAC = apixaban, dabigatran, or rivaroxaban.

†Other = enoxaparin or clopidogrel.

Table 2 Procedural characteristics

Cryoballoon freeze characteristic	Mean	SEM	SD	*P*
No. of freeze applications				
LSPV	2.3	0.1	0.7	
LIPV	2.0	0	0	.012*
RSPV	2.1	0.1	0.5	
RIPV	2.5†	0.2	1.3	
Freeze duration (s)				
LSPV (n = 101)	169.3	2.8	28.5	
LIPV (n = 68)	178.1†	1.2	10.0	.001*
RSPV (n = 92)	158.5†	4.0	38.2	
RIPV (n = 109)	168.5	3.0	31.2	
Nadir temperature (°C)				
LSPV (n = 101)	−47.2†	−0.7	−7.1	
LIPV (n = 68)	−44.8	−0.8	−6.8	.001*
RSPV (n = 92)	−48.3†	−0.7	−7.1	
RIPV (n = 109)	−45.0	−0.6	−6.4	
Procedure time (min)	126.4	3.5	22.7	
LA dwell time (min)	80.6	2.6	16.7	
Fluoroscopy time (min)	16.4	1.2	7.5	
IV saline fluid use (mL)	1418.8	79.9	505.4	
Radiopaque contrast (mL)	45.5	4.2	25.3	

IV = intravenous; LA = left atrial; LIPV = left inferior pulmonary vein; LSPV = left superior pulmonary vein; RIPV = right inferior pulmonary vein; RSPV = right superior pulmonary vein.
*Significant *P* value.
†The outlier group(s).

ANOVA test ($P = .001$). Mean procedure time, LA dwell time, and fluoroscopy time were recorded as 126 (±23 SD; median 121; mode 120), 80 (±17 SD; median 80; mode 60), and 16 (±8 SD; median 15; mode 19) minutes, respectively.

LA measurements of pre- and postablation cardiac dimensions are reported in Table 3. Left- and right-sided LA ablation procedures were not statistically different ($P = .935$), and each had a mean posterior LA wall surface area of ablation of 11.4 (±5.3 SD; median 10; mode 9) and 11.3 (±5.2 SD; median 10; mode 8) cm^2, respectively (Figure 3). On average, the total posterior LA wall surface area was 31.1 (±10.2 SD; median 30; mode 37) cm^2, and the mean surface area of the nonablated posterior wall was 8.4 (±8.2 SD; median 6; mode 6) cm^2, which was typically a vertical rectangular-shaped zone in most patients (Figures 1A and 3B). In total, 27% (±21.9% SD) of the posterior LA wall remained electrically intact and unablated. The total area of posterior wall ablation was 22.7 (±10.1 SD) cm^2; by comparison, each cryoballoon has a 2-dimensional contact area of 6.15 cm^2 when measuring from the tip to the equator of the cryoballoon (in the 28-mm cryoballoon). The distribution zone of the liquid nitrous oxide within the second-generation cryoballoon encompasses a surface area from the distal nose tip to the equator of the balloon. Consequently, the hypothetical contact surface area of 4 PVs calculated in the 28-mm cryoballoon is 24.6 cm^2, which is in close approximation of the 22.7 cm^2 mean ablation area that was reported in this study (Figure 4).

Table 3 LA measurements of pre- and postablation cardiac dimensions

LA dimension measurement	Mean	SEM	SD
Preablation: posterior LA wall surface area (cm^2)	31.1	1.6	10.2
Postablation: posterior LA wall surface area (cm^2)			
Left-sided	11.4	0.8	5.3
Right-sided	11.3	0.8	5.2
Postablation: posterior LA wall not ablated Central zone surface area (cm^2)	8.4	1.3	8.2
Postablation: distance from the PV to the ablation edge (cm)	1.9	0.1	0.7

LA = left atrium; PV = pulmonary vein.

As shown in Table 3, the measured distance from the proximal PV to the cryoballoon PVI ablation edge had a mean value of 1.9 (±0.7 SD; median 1.8; mode 1.8) cm, which had a 1-to-1 relationship with the approximately 2-cm distance (from the nose tip to the equator of the cryoballoon) that was available for ablation in the 28-mm Arctic Front Advance cryoballoon. When measured at each PV, the distance from the PV to the ablation edge had a mean value of 1.7 (±0.7 SD; median 1.7; mode 1.9), 1.7 (±0.6 SD; median 1.6; mode 1.5), 1.8 (±0.7 SD; median 1.6; mode 1.6), and 2.3 (±0.7 SD; median 2.3; mode 1.8) cm for the LPSV, LIPV, RSPV, and RIPV, respectively. Using the ANOVA test, we found that the RIPV had a statistically longer distance from the PV to the PVI ablation edge ($P = .001$).

After the completion of this study, all 43 patients had undergone electrophysiology examination at 1, 3, and 6 months postablation with ambulatory cardiac monitoring. Two patients had a recurrence of AF, and 41 patients (out of

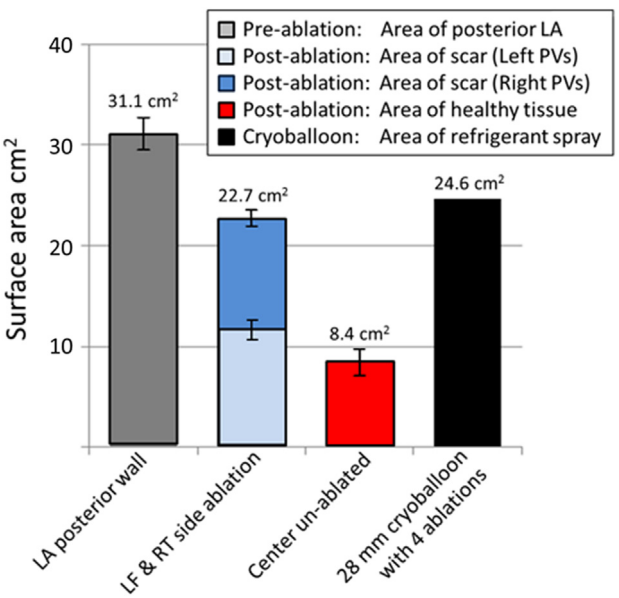

Figure 4 Bar graph of the mean posterior left atrial (LA) wall surface areas in 43 patients (gray bar). After cryoballoon ablation, the posterior LA wall had a central zone that was unablated (red bar). This nonablated zone (red bar) was 27% of the posterior LA wall on average, and there was no statistical difference between areas of left- and right-sided ablation procedures (blue bars; $P = .935$). The black bar represents the surface area of the refrigerant spray (from the distal nose tip to the equator of the cryoballoon) in the 28-mm cryoballoon. Error bars represent ±1 SEM. LF = left; PV = pulmonary vein; RT = right.

43 total patients) had no AF at 6 months with a single procedure (95.3% freedom from AF). The mean follow-up period was 9.2 (±2.1 SD; range 6–13) months for the entire patient cohort.

Discussion

To date, this study is the first quantitative examination of the ablative lesion set created by the second-generation cryoballoon, and in this study, we exclusively used the 28-mm Arctic Front Advance cryoballoon catheter in 43 consecutive patients. By using only the 28-mm second-generation cryoballoon in 43 consecutive patients, we have established the quantitative spatial measurements of the WACA lesion sets created by cryoablation under current and typical usage patterns, which were in agreement with a recent multicenter examination of cryoballoon procedural measurements.[20] The antral lesion placement creates an ablation set that leaves 27% of the posterior LA wall intact. This LA debulking by the cryoballoon catheter may have a beneficial outcome with regard to longer-term efficacy. When measuring distance from the PV to the ablation edge, the RIPV had a statistically longer mean distance (2.3 cm) in this study than did the other 3 PVs. Interestingly, the RIPV also had a statistically higher mean number of freeze applications than did the other 3 PVs. By comparison, the LIPV had the longest mean freeze duration and the RSPV had the lowest mean nadir temperature.

Two small studies[18,19] have been previously published for the first-generation cryoballoon system. In the study by Chierchia et al,[18] the researchers examined 8 patients (4 treated with the 23-mm cryoballoon and 4 treated with the 28-mm cryoballoon). Although limited surface area calculations were reported, this study found an approximately 2-cm linear zone of ablation that surrounds each PV while using 3D EAM measurements, which was similar to the 1.9-cm distance recorded in the present study. In addition, the lesion created with the 28-mm cryoballoon was more antral in position when compared statistically with the 23-mm cryoballoon lesion. On average, the lesions in the study by Chierchia et al were created with 5-minute cryoablation applications and 2 ablation procedures per PV, with a target nadir temperature of lower than −40°C. These longer application times were typical usage patterns during the usage of the first-generation cryoballoon because of limited cryo-refrigerant distribution in the first-generation balloon.

By comparison, an earlier study by Reddy et al[19] evaluated 8 patients treated only with the 23-mm first-generation cryoballoon. By using a 3D EAM protocol similar to that used in our study and the study by Chierchia et al, Reddy et al found that the lesion sets resided near the PV ostium with little antral penetration by the cryoablation lesion set. Since the original publication of the results of Reddy et al, there has been a predominant usage of the 28-mm cryoballoon because of the ability to create an antral lesion set and the perceived potential to reduce the incidence rate of PV stenosis. More recently, physicians have adopted a typical usage strategy that reserves the usage of the 23-mm cryoballoon to patients in whom all PVs have a measured diameter of less than approximately 16 mm. In cases where there are mismatched vein sizes, the 28-mm cryoballoon is used singularly when any PV has a diameter of 18 mm or greater because of the larger freezing surface area in the second-generation cryoballoon, which covers small and large PVs. Interestingly, by current "typical" physician usage, all 8 patients in the study by Reddy et al would have been ablated with the 28-mm cryoballoon. At present, more than 80% of all cryoballoon usage is with the 28-mm balloon (Medtronic data).

Since the original surgical Cox Maze procedure, intracardiac ablation strategies have been worked out to recreate a safe and durable lesion set for the treatment of AF. The Haïssaguerre PVI strategy has been successful in many patients with AF. More recently, some specific strategies of substrate ablation have proved to be interesting, including ganglionic plexus[21,22] and rotor ablation procedures.[23,24] While we await more trial data, it is interesting that this second-generation cryoballoon creates lesions that are near the ganglionic plexi on the LA posterior wall.[21] Additionally many stable rotors have been found near the "PV ostia-to-LA antrium" border which is contiguous with the area of cryoballoon ablation.[24] Consequently, recent improved 1-year outcomes with the second-generation cryoballoon may reflect this lesion set that is wide and circumferential, as denoted by the present study. With the second-generation cryoballoon system, 5 independent published studies have demonstrated a 12-month efficacy of 80% or more.[17,25–28] Two of these studies had a comparator arm with the first-generation cryoballoon and demonstrated an 18%–20% improvement in efficacy.[17,25]

However, with a wider lesion set, more care is necessary to avoid collateral tissue damage near the posterior LA wall, including the phrenic nerve. Compared to radiofrequency catheter ablation, the cryoballoon lesion enhances the risk of phrenic nerve injury (PNI), both transient and longer-term.[2,5] More recent phrenic nerve monitoring techniques have lowered the risk of PNI,[29] but the increased occurrence of PNI during a cryoballoon ablation compared to RF ablation for PVI is both a consequence of and evidence for the wide and transmural cryoballoon lesion set.

Study limitations

To minimize user variation in cryoballoon handling during this study, all cryoballoon ablation procedures were conducted by 1 experienced physician. This study design allowed for a robust measure in multiple patients and reported mean values; however, the design did not allow for the culmination of multiple user experience with the cryoballoon. In addition, we do not know the surface area measurements of the cryoballoon lesion set at 6–12 months.

Conclusion

This study has demonstrated the WACA lesion formation that is observable acutely by using 3D electroanatomic

mapping after cryoballoon ablation. Left- and right-sided areas of ablation were similar. Acutely after ablation, 27% of the posterior LA wall remained intact and electrically conductive. At 6 months postablation, 95.3% of all patients remained free of AF with a single cryoablation procedure.

Even with a geometrically derived ablation volume, the cryoballoon catheter was able to form a WACA lesion set. The earlier usage of the first-generation cryoballoon was constrained by the limited balloon surface coverage of the cryo-refrigerant and by selective usage of the 23-mm cryoballoon, which led to a lesion set near the PV ostium.

References

1. January CT, Wann LS, Alpert JS, et al. 2014 AHA/ACC/HRS Guideline for the Management of Patients With Atrial Fibrillation: a report of the American College of Cardiology/American Heart Association Task Force on Practice Guidelines and the Heart Rhythm Society. J Am Coll Cardiol 2014;64:e1–e76.
2. Calkins H, Kuck KH, Cappato R, et al. 2012 HRS/EHRA/ECAS Expert Consensus Statement on Catheter and Surgical Ablation of Atrial Fibrillation: recommendations for patient selection, procedural techniques, patient management and follow-up, definitions, endpoints, and research trial design. Europace 2012;14:528–606.
3. Fuster V, Rydén LE, Cannom DS, et al. 2011 ACCF/AHA/HRS focused updates incorporated into the ACC/AHA/ESC 2006 guidelines for the management of patients with atrial fibrillation: a report of the American College of Cardiology Foundation/American Heart Association Task Force on practice guidelines. Circulation 2011;123:e269–e367.
4. Haïssaguerre M, Jaïs P, Shah DC, Takahashi A, Hocini M, Quiniou G, Garrigue S, Le Mouroux A, Le Métayer P, Clémenty J. Spontaneous initiation of atrial fibrillation by ectopic beats originating in the pulmonary veins. N Engl J Med 1998;339:659–666.
5. Packer DL, Kowal RC, Wheelan KR, Irwin JM, Champagne J, Guerra PG, Dubuc M, Reddy V, Nelson L, Holcomb RG, Lehmann JW, Ruskin JN; STOP AF Cryoablation Investigators. Cryoballoon ablation of pulmonary veins for paroxysmal atrial fibrillation: first results of the North American Arctic Front (STOP AF) pivotal trial. J Am Coll Cardiol 2013;61:1713–1723.
6. Van Belle Y, Janse P, Rivero-Ayerza MJ, Thornton AS, Jessurun ER, Theuns D, Jordaens L. Pulmonary vein isolation using an occluding cryoballoon for circumferential ablation: feasibility, complications, and short-term outcome. Eur Heart J 2007;28:2231–2237.
7. Schilling RJ, Kadish AH, Peters NS, Goldberger J, Davies DW. Endocardial mapping of atrial fibrillation in the human right atrium using a non-contact catheter. Eur Heart J 2000;21:550–564.
8. Voss F, Steen H, Bauer A, Giannitsis E, Katus HA, Becker R. Determination of myocardial infarct size by noncontact mapping. Heart Rhythm 2008;5:308–314.
9. Knackstedt C, Schauerte P, Kirchhof P. Electro-anatomic mapping systems in arrhythmias. Europace 2008;10:iii28–iii34.
10. Gupta S, Desjardins B, Baman T, Ilg K, Good E, Crawford T, Oral H, Pelosi F, Chugh A, Morady F, Bogun F. Delayed-enhanced MR scar imaging and intraprocedural registration into an electroanatomical mapping system in post-infarction patients. JACC Cardiovasc Imaging 2012;5:207–210.
11. Wieczorek M, Hoeltgen R. Right atrial tachycardias related to regions of low-voltage myocardium in patients without prior cardiac surgery: catheter ablation and follow-up results. Europace 2013;15:1642–1650.
12. Parmar BR, Jarrett TR, Burgon NS, Kholmovski EG, Akoum NW, Hu N, Macleod RS, Marrouche NF, Ranjan R. Comparison of left atrial area marked ablated in electroanatomical maps with scar in MRI. J Cardiovasc Electrophysiol 2014;25:457–463.
13. Daccarett M, McGann CJ, Akoum NW, MacLeod RS, Marrouche NF. MRI of the left atrium: predicting clinical outcomes in patients with atrial fibrillation. Expert Rev Cardiovasc Ther 2011;9:105–111.
14. McGann C, Akoum N, Patel A, et al. Atrial fibrillation outcome is predicted by left atrial remodeling on MRI. Circ Arrhythm Electrophysiol 2014;7:23–30.
15. Daccarett M, Badger TJ, Akoum N, Burgon NS, Mahnkopf C, Vergara G, Kholmovski E, McGann CJ, Parker D, Brachmann J, Macleod RS, Marrouche NF. Association of left atrial fibrosis detected by delayed-enhancement magnetic resonance imaging and the risk of stroke in patients with atrial fibrillation. J Am Coll Cardiol 2011;57:831–838.
16. Marrouche NF, Wilber D, Hindricks G, et al. Association of atrial tissue fibrosis identified by delayed enhancement MRI and atrial fibrillation catheter ablation: the DECAAF study. JAMA 2014;311:498–506.
17. Fürnkranz A, Bordignon S, Dugo D, Perotta L, Gunawardene M, Schulte-Hahn B, Nowak B, Schmidt B, Chun JK. Improved 1-year clinical success rate of pulmonary vein isolation with the second-generation cryoballoon in patients with paroxysmal atrial fibrillation. J Cardiovasc Electrophysiol 2014;25:840–844.
18. Chierchia GB, de Asmundis C, Sorgente A, Paparella G, Sarkozy A, Müller-Burri SA, Capulzini L, Yazaki Y, Brugada P. Anatomical extent of pulmonary vein isolation after cryoballoon ablation for atrial fibrillation: comparison between the 23 and 28 mm balloons. J Cardiovasc Med (Hagerstown) 2011;12:162–166.
19. Reddy VY, Neuzil P, d'Avila A, Laragy M, Malchano ZJ, Kralovec S, Kim SJ, Ruskin JN. Balloon catheter ablation to treat paroxysmal atrial fibrillation: what is the level of pulmonary venous isolation? Heart Rhythm 2008;5:353–360.
20. DeVille JB, Svinarich JT, Dan D, Wickliffe A, Kantipudi C, Lim HW, Plummer L, Baker J, Kowalski M, Baydoun H, Jenkins M, Chang-Sing P. Comparison of resource utilization of pulmonary vein isolation: cryoablation versus RF ablation with three-dimensional mapping in the Value PVI study. J Invasive Cardiol 2014;26:268–272.
21. Katritsis DG, Pokushalov E, Romanov A, Giazitzoglou E, Siontis GC, Po SS, Camm AJ, Ioannidis JP. Autonomic denervation added to pulmonary vein isolation for paroxysmal atrial fibrillation: a randomized clinical trial. J Am Coll Cardiol 2013;62:2318–2325.
22. Zhou J, Scherlag BJ, Edwards J, Jackman WM, Lazzara R, Po SS. Gradients of atrial refractoriness and inducibility of atrial fibrillation due to stimulation of ganglionated plexi. J Cardiovasc Electrophysiol 2007;18:83–90.
23. Baykaner T, Lalani GG, Schricker A, Krummen DE, Narayan SM. Mapping and ablating stable sources for atrial fibrillation: summary of the literature on Focal Impulse and Rotor Modulation (FIRM). J Interv Card Electrophysiol 2014;40:237–244.
24. Narayan SM, Baykaner T, Clopton P, Schricker A, Lalani GG, Krummen DE, Shivkumar K, Miller JM. Ablation of rotor and focal sources reduces late recurrence of atrial fibrillation compared with trigger ablation alone: extended follow-up of the CONFIRM trial (Conventional Ablation for Atrial Fibrillation With or Without Focal Impulse and Rotor Modulation). J Am Coll Cardiol 2014;63:1761–1768.
25. DI Giovanni G, Wauters K, Chierchia GB, et al. One-year follow-up after single procedure cryoballoon ablation: a comparison between the first and second generation balloon. J Cardiovasc Electrophysiol 2014;25:834–839.
26. Chierchia GB, Di Giovanni G, Ciconte G, et al. Second-generation cryoballoon ablation for paroxysmal atrial fibrillation: 1-year follow-up. Europace 2014;16:639–644.
27. Metzner A, Reissmann B, Rausch P, et al. One-year clinical outcome after pulmonary vein isolation using the second-generation 28-mm cryoballoon ablation. Circ Arrhythm Electrophysiol 2014;7:288–292.
28. Aryana A, Morkoch S, Bailey S, Lim HW, Sara R, d'Avila A, O'Neill PG. Acute procedural and cryoballoon characteristics from cryoablation of atrial fibrillation using the first- and second-generation cryoballoon: a retrospective comparative study with follow-up outcomes. J Interv Card Electrophysiol 2014;41:177–186.
29. Lakhani M, Saiful F, Parikh V, Goyal N, Bekheit S, Kowalski M. Recordings of diaphragmatic electromyograms during cryoballoon ablation for atrial fibrillation accurately predict phrenic nerve injury. Heart Rhythm 2014;11:369–374.

CLINICAL PERSPECTIVES

This study is the first demonstration of the acute ablation zone that is established after cryoablation with the new Arctic Front Advance cryoballoon catheter. Because of an increased area of refrigerant distribution in the new balloon, users will find that the established pulmonary vein isolation lesion set is a wide area circumferential ablation. The remaining (intact) posterior left atrial wall is electrically conductive and approximately 27% of the original surface area, and the border demarcation between ablated and nonablated cardiac tissue demonstrates a sharp voltage gradient, which may be indicative of acute transmural lesion formation.

This larger area of antral ablation may explain (in part) the improved 12-month efficacy that is observed with the new cryoballoon, as 5 independent studies have reported more than 80% freedom from AF. It is well established that there is a prevalence of electrical disruption (eg, rotors and ganglionic plexi) on the posterior left atrial wall that can severe as triggers/propagators/sustainers for AF. However, the new cryoballoon must be used with a refinement in procedural application (mainly reduced freeze dosing/duration). Phrenic nerve injury is still possible with the second-generation cryoballoon, and novel monitoring techniques may provide better surveillance of impending damage. In this study, cryoballoon freeze applications were typically less than 3 minutes, and by comparison, older reports on first-generation cryoballoon have used 5-minute applications. More than 90% freedom from AF, at 6 months in this study, indicates that these shorter freeze applications are still effective.